

## Research paper

Changes in the amide I FT-IR bands of poly-L-lysine  
on spray-drying from  $\alpha$ -helix,  $\beta$ -sheet or random coil conformations

Alexander Maurer, Geoffrey Lee \*

Department of Pharmaceutics, Friedrich-Alexander-University, Erlangen, Germany

Received 13 April 2005; accepted in revised form 12 August 2005

Available online 10 October 2005

## Abstract

Poly-L-lysine (PLS) was spray-dried in a laboratory-scale, mini spray-dryer at  $T_{in}/T_{out}=150/90-95\text{ }^{\circ}\text{C}$  from three different liquid feeds composed mainly of  $\alpha$ -helix,  $\beta$ -sheet or random coil conformations of the homopolypeptide. FT-IR analysis of the liquid feeds, the spray-dried solids, and the re-dissolved solids was performed by considering the deconvoluted and second-derivative amide I spectra, as well as a Gaussian curve fitting procedure. All three initial conformations were transformed by spray-drying to anti-parallel  $\beta$ -sheet with bands at 1623 and 1690  $\text{cm}^{-1}$ . The  $\beta$ -sheet liquid feed showed a band at 1616  $\text{cm}^{-1}$  indicating a denatured, extended chain structure that was also converted to anti-parallel  $\beta$ -sheet on spray-drying. The shift to  $\beta$ -sheet cannot therefore be a simple result of forming the conformation with the strongest H-bonds in the dried state. We suggest that steric effects arising from the close approach of the globular polypeptide molecules during drying make the anti-parallel  $\beta$ -sheet structure energetically favorable in the solid state. This suggestion is supported by the effects of trehalose on the FT-IR amide I bands of the spray-dried PLS. No stabilizing effects were observed on either the initial  $\alpha$ -helix or  $\beta$ -sheet (extended chain) conformations. Random coil could be partially stabilized. Again, no direct relation to H-bond strength is evident. The efficacy of the trehalose could be related to the ability of newly-formed trehalose/PLS intermolecular H-bonds to stabilize the intramolecular H-bonds of the secondary structural elements.

© 2005 Published by Elsevier B.V.

Keywords: Poly-L-lysine; Spray-drying; FT-IR; Amide I; Trehalose; Hydrogen bonding

## 1. Introduction

It is not surprising that proteins show changes in their structural conformations on drying. Water molecules play an important role in the maintenance of a globular protein's native form [1] and its removal can lead, for example, to loss of enzymatic activity [2] or aggregation [3]. Fourier transformation infra-red spectroscopy (FT-IR) has been used to help elucidate the changes in secondary structure of proteins that take place during drying. Using this technique Prestrelski et al. [4] identified three types of behavior of a protein during freeze-drying. It can either retain native confirmation on drying and re-hydration, or (partially) unfold during drying but refold to the native form on re-hydration, or irreversibly unfold on drying. These authors also reported second-derivative spectral

changes of poly-L-lysine (PLS) during freeze-drying. This homopolypeptide adopts in aqueous solution either an  $\alpha$ -helix,  $\beta$ -sheet or random coil conformation in dependence of pH and temperature [5]. Each of these three conformations altered during freeze-drying to a more predominant  $\beta$ -sheet structure in the solid state. The  $\beta$ -sheet conformation is energetically more favorable than either the  $\alpha$ -helix or random coil in the dried solid because it has the strongest H-bonds and requires therefore a lower degree of solvation than the other two conformations [6].

It has been claimed that this general conformational shift to enhanced  $\beta$ -sheet during drying of a protein solution depends on the rate of drying. Volkers et al. [7] found that slow air-drying of droplets of an aqueous PLS solution of initial random coil conformation produced  $\beta$ -sheet conformation. Rapid air-drying produced, however, retention of the original random coil conformation. These authors concluded that drying rate has a major influence on retention of native structure. If this were the case, then the spray-drying of a protein solution should be particularly propitious for maintaining protein native form, since droplet drying in a laboratory-scale micro spray-dryer is completed in  $\ll 1000\text{ ms}$  [8]. There is, however, little published work on the changes in protein secondary structure

\* Corresponding author. Department of Pharmaceutics, Friedrich-Alexander-University, Cauerstr. 4, 91058 Erlangen, Germany. Tel.: +49 9131 85295 52; fax: +49 9131 85295 45.

E-mail address: [lee@pharmtech.uni-erlangen.de](mailto:lee@pharmtech.uni-erlangen.de) (G. Lee).

that occur during spray-drying. The spray-drying of lysozyme produced a reduction in the intensity of the native  $\alpha$ -helix bands in the second derivative amide I spectrum of the solid compared with the liquid feed [9]. Spray-dried immunoglobulin G showed minimal change in its amide I deconvoluted spectrum after spray-drying [10,11]. Spray-dried salmon Calcitonin plus mannitol showed loss of  $\alpha$ -helix bands in the second derivative amide I spectrum on storage [12]. These few studies are clearly not a basis to substantiate a kinetic dependence of band perturbations during spray-drying of a protein.

We have conducted a systematic study of the band perturbations occurring during spray-drying of aqueous solutions of PLS. In contrast to freeze-drying [4] there has been no published study of the spray-drying of PLS. We have employed FT-IR spectroscopy to examine the effects of spray-drying on initial  $\alpha$ -helix,  $\beta$ -sheet and random coil secondary structures of this homopolypeptide. In this paper we consider the deconvoluted amide I spectra, as well as the second-derivative spectra and Gaussian curve fitting of the deconvoluted spectra. Additionally, the effects of the adjuvant trehalose on the spray-drying-induced changes in the amide I spectra were examined. Since, trehalose is thought to form H-bonds with proteins during a drying process ('water replacement'), we anticipated differential effects of the trehalose on the three secondary structural elements depending on their H-bonding ability [6]. We seek therefore a possible relationship between type and strength of H-bonds, and the effectivity of trehalose in ameliorating band perturbation of  $\alpha$ -helix,  $\beta$ -sheet and random coil structures during spray-drying. Our results demonstrate such differential effects, although not of the nature first anticipated.

## 2. Materials and methods

### 2.1. Materials

PLS (molecular weight = 30 kDa) and trehalose dihydrate were all supplied from Sigma Chemicals, Munich, and were used as received. Water was freshly double-distilled from an all-glass apparatus.

### 2.2. Spray drying

#### 2.2.1. Preparation of liquid feed

Predominant secondary structural elements of PLS existing in aqueous solution can be produced by adjusting the pH and the use of heat [5]. PLS was first dissolved in water to give a 5% w/v solution. The predominantly  $\alpha$ -helix conformation was obtained by adjusting the pH to 10.8 using 1 M NaOH. The predominantly  $\beta$ -sheet form required adjustment of the pH to 11.5 and heating at 60 °C for 30 min. The predominantly random coil conformation was obtained by adjusting the pH to 7.8 using the 1 M NaOH. These three initial solutions are referred to as the ' $\alpha$ -helix' liquid feed, the ' $\beta$ -sheet' liquid feed, and the 'random coil' liquid feed. Trehalose was added to the liquid feed solution, as required.

### 2.3. Spray-drying

Each 5% w/v PLS aqueous solution was spray-dried using a Büchi B-191 laboratory micro spray-drier. This was fitted with a high efficiency cyclone to maximize powder yield, as fully described before [13]. Five to 10 ml of the liquid feed were than spray-dried under the following process conditions: inlet and outlet air temperatures,  $T_{in}/T_{out}=150/92-95$  °C; drying air flow rate,  $v_{da}=600$  L/min; liquid feed flow rate,  $v_{lf}=3$  mL/min; atomizing air flow rate,  $v_{aa}=700$  L/h. Each spray-dried powder was removed from the cyclone's collecting vessel and immediately transferred to a small, screw-capped glass vial and stored under  $N_2$  at  $-80$  °C until examination.

### 2.4. Fourier transformation infra-red spectroscopy (FT-IR)

The FT-IR spectra of both liquid and solid samples were obtained using a Nicolet Magna IR 550 FT-IR spectrometer. Liquid samples containing 5% w/v of the PLS were examined in a thermostatted, specially constructed  $CaF_2$  window of fixed sample layer thickness 5.6  $\mu m$  [14]. Solid samples were produced by pressing KBr windows (1.5 mg protein + up to 200 mg KBr) on a Carver press at 5–6 T pressure. 152 spectra were recorded per sample at a sensitivity of 4  $cm^{-1}$ . For the liquid samples, a water spectrum was first subtracted from the sample spectrum using the Nicolet Omnic software. All subsequent manipulations of the original spectra were performed using Galactic Grams software. The amide I band range between 1580–1720  $cm^{-1}$  was first isolated from the complete (difference) spectrum using the 'Zap' option with baseline correction, and a Fourier self-deconvolution (FSD) for band narrowing ( $\gamma=3$ , 60% smoothing) then performed. Individual peak positions were identified from consideration of both the deconvoluted spectrum and the second-derivative spectrum of this range. The 'Peak fitting' procedure was then applied to the deconvoluted (difference) spectrum to resolve and quantify its individual, component bands according to a Gaussian curve fit (GCF).

## 3. Results and discussion

The spray-drying experiments and FT-IR analyses reported here were performed three times using the same process conditions and FSD/GCF parameters. The latter can substantially influence the number, position and intensity of the bands resolved by GCF [15]. The FSD parameters could always be held constant for both liquid and solid samples. The GCF parameters had to be varied to give the best least-squares fit of the individual bands to each deconvoluted spectrum. One must recognize that this variation can influence the properties of the resolved bands. We preferred, however, our combined FSD/second-derivative/GCF approach to any attempt at quantitative analysis of the second derivative spectra alone. The reader is referred to the critical review articles [16,17].

### 3.1. Poly-L-lysine

Fig. 1(a)–(c) show the deconvoluted amide I spectra, the GCF bands thereof, and the second-derivative spectra of the three aqueous PLS solutions used as liquid feeds. The second-derivative band positions agree well with the previous data of

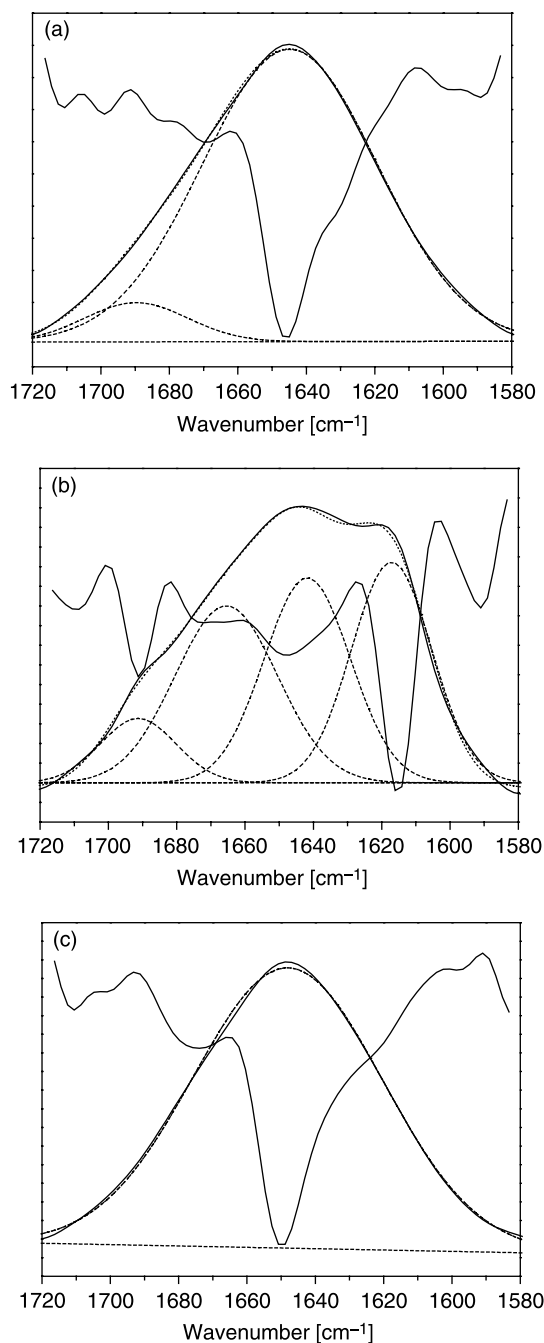


Fig. 1. Amide I spectra of aqueous PLS solutions used as liquid feeds for spray-drying experiments. In each figure the top, downwards-reaching curve is the second derivative spectrum and the lower, upwards-reaching curves are the deconvoluted spectrum plus curve fitted, deconvoluted spectrum and resolved individual bands. (a) Liquid feed prepared at pH 7.8 giving  $\alpha$ -helix conformation; (b) liquid feed prepared at pH 10.8 plus 30 min at 80 °C giving  $\beta$ -sheet conformation; (c) liquid feed prepared at pH 12.8 giving random coil conformation.

Prestrelski et al. [4] who reported aqueous  $\alpha$ -helix with a strong band at 1645  $\text{cm}^{-1}$ ,  $\beta$ -sheet with a strong band at 1619  $\text{cm}^{-1}$  and a weaker band at 1692  $\text{cm}^{-1}$ , and random coil with a strong band at 1649  $\text{cm}^{-1}$ . The second-derivative spectrum of the  $\alpha$ -helix liquid feed in Fig. 1(a) shows a single, broad band at 1644  $\text{cm}^{-1}$  with a shoulder at 1630  $\text{cm}^{-1}$  and two weak bands at approximately 1670 and 1680  $\text{cm}^{-1}$ . The deconvoluted spectrum also shows a broad band centered at 1644  $\text{cm}^{-1}$  assignable to  $\alpha$ -helix conformation [4]. Neither the shoulder at 1630  $\text{cm}^{-1}$  nor the weak band at 1670  $\text{cm}^{-1}$  in the second derivative spectrum is, however, evident in the deconvoluted spectrum and they are also not resolved by the GCF. Only a small, non-assignable band centered at 1691  $\text{cm}^{-1}$  is resolved in the GCF. The quantitative analysis for the relative areas under the bands of the GCF result is given in Table 1 and yields 93%  $\alpha$ -helix conformation. The second-derivative spectrum of the  $\beta$ -sheet liquid feed in Fig. 1(b) shows two bands at 1616 and 1688  $\text{cm}^{-1}$ , the former being the stronger. A broad band is also seen at 1647  $\text{cm}^{-1}$ . The deconvoluted spectrum is clearly comprised of a number of bands, with peaks being evident at approximately 1615, 1690, and 1645  $\text{cm}^{-1}$ . The GCF resolves three bands at approximately the same wavenumbers, plus a further band at 1670  $\text{cm}^{-1}$ . The position of the 1617  $\text{cm}^{-1}$  band indicates strong intermolecular H-bonds existing in extended, denatured polypeptide chains [16]. The additional, high-frequency band at 1691  $\text{cm}^{-1}$  comes from transition dipole coupling of a  $\beta$ -sheet structure [18]. The heat-induced transition of  $\alpha$ -helix to  $\beta$ -sheet of aqueous PLS is known to yield bands at 1618 and 1693  $\text{cm}^{-1}$  [19]. The assignment of the 1617 and 1691  $\text{cm}^{-1}$  bands to  $\beta$ -sheet structure [15] yields from the GCF relative intensities of 30 and 8.3%, respectively (Table 1). The 1642  $\text{cm}^{-1}$  band seen in both the second-derivative and deconvoluted spectra is assigned to  $\alpha$ -helix. Its relative intensity of 30% (Table 1) represents that fraction of the original  $\alpha$ -helix structure from the pH 11.5 solution that was evidently not converted by heating to  $\beta$ -sheet. The heat-induced transition of  $\alpha$ -helix to  $\beta$ -sheet of aqueous PLS is indeed a kinetic process [19], and the 30 min duration of heating at 60 °C used here did not cause complete change to  $\beta$ -sheet. The GCF also resolves a fourth band at 1670  $\text{cm}^{-1}$  that is only weakly evident in the second-derivative spectrum and barely visible in the deconvoluted spectrum. Bands in this range can be assigned to non-H-bonded amide groups within turn structures [16]. The result of the GCF in Table 1 yields therefore approximately 38%  $\beta$ -sheet conformation and 30% helix. The random coil liquid feed gives a second-derivative spectrum in Fig. 1(c) having a strong band at 1650  $\text{cm}^{-1}$  with a shoulder at 1620  $\text{cm}^{-1}$  and a second weak band at approximately 1675  $\text{cm}^{-1}$ . The deconvoluted spectrum shows, however, only a single band with absorption maximum at 1651  $\text{cm}^{-1}$  and no sign of other smaller peaks. Accordingly, the GCF resolves only this single band, giving a quantitative result of 100% random coil structure (Table 1). Circular dichroism studies of aqueous poly-L-lysine [20] have indicated that at room temperature up to 50% of a left-handed trans polyproline II conformation exists in this solution. There have, however, been no FT-IR studies of this phenomenon. Note that

Table 1  
Gaussian curve-fitting (GCF) of amide I spectra from PLS liquid feeds, spray-dried solids and re-dissolved powders

System	Liquid feed	Peak Nr.	Wavenumber GCF (cm <sup>-1</sup> )	Wavenumber 2nd derivative (cm <sup>-1</sup> )	$\alpha$ -helix (%)	$\beta$ -sheet (%)	Random coil (%)	other (%)
Liquid feed	$\alpha$ -helix	1	1690	1681				7
		2	1644	1644	93			
		Total			93			7
SD	$\alpha$ -helix	1	1692	1693		13		
		2	1655	1655			41	
		3	1627	1627		46		
		Total				59	41	
Re-dissolved	$\alpha$ -helix	1	1676	1675				27
		2	1645	1646	49			
		3	1620	1625		24		
		Total			49	24		27
Liquid feed	$\beta$ -sheet	1	1691	1688		8		
		2	1665	1670				31
		3	1642	1647	30			
		4	1617	1616		30		
		Total			30	38		31
SD	$\beta$ -sheet	1	1693	1693		9		
		2	1673	1675				30
		3	1655	1657			8	
		4	1627	1625		53		
		Total				62	8	30
Re-dissolved	$\beta$ -sheet	1	1691	1691		13		
		2	1669	1670				23
		3	1650	1651			(16)	
		4	1636	1631		(18)		
		5	1619	1616		31		
		Total				62	(16)	18
Liquid feed	Random coil	1	1651	1650			100	
		Total					100	
SD	Random coil	1	1694	1694		5		
		2	1672	1675				19
		3	1653	1656			17	
		4	1641	1640	(3)			
		5	1625	1621		56		
		Total			(3)	61	17	19
Re-dissolved	Random coil	1	1648	1649			98	
		2	1633	1633		2		
		Total				2	98	

the major bands in Fig. 1(a)–(c) lie some 3–6 cm<sup>-1</sup> higher than those originally reported by Jackson et al. for PLS [5] because of wavenumber downshifting in the D<sub>2</sub>O used by these authors.

The solid PLS samples obtained after spray-drying the three different liquid feeds all show second-derivative and deconvoluted spectra that are predominately of the  $\beta$ -sheet type. In Fig. 2(a) the original second-derivative band at 1644 cm<sup>-1</sup> of the  $\alpha$ -helix liquid feed has completely disappeared, to be replaced by strong bands at 1627 and 1693 cm<sup>-1</sup>. These are characteristic of intramolecular H-bonds of the anti-parallel  $\beta$ -sheet conformation [17]. A weak band at 1655 cm<sup>-1</sup> lies closer to the expected position of random coil (1650 cm<sup>-1</sup> in Fig. 1(c)) than of  $\alpha$ -helix (1644 cm<sup>-1</sup> in Fig. 1(a)), although Prestrelski [4] assigned a similar band after freeze-drying of PLS to residual  $\alpha$ -helix. The deconvoluted spectrum of this spray-dried solid also shows a greatly altered shape compared with that of the  $\alpha$ -helix liquid feed. The two peaks seen at 1627 and 1692 cm<sup>-1</sup> correspond almost exactly to those seen in the second derivative spectrum and are assignable to anti-parallel

$\beta$ -sheet [17]. The presence of a third peak at 1655 cm<sup>-1</sup> is also evident, as already seen in the second derivative spectrum. The GCF resolves three bands at the same wavenumbers, viz. 1627, 1692 and 1655 cm<sup>-1</sup>, giving therefore agreement between second derivative and deconvoluted spectra, and also GCF. There is no indication or resolution of a residual  $\alpha$ -helix band at around 1644 cm<sup>-1</sup> in any of the spectra, as the 1655 cm<sup>-1</sup> band is too far removed. The quantitative GCF result yields therefore 59%  $\beta$ -sheet and 41% random coil (Table 1), clearly much changed from the 93%  $\alpha$ -helix in the initial liquid feed. Spray drying has therefore induced a complete transition from  $\alpha$ -helix to  $\beta$ -sheet plus random coil structures.

The spray-dried solid obtained from the  $\beta$ -sheet liquid feed retains a second-derivative spectrum of  $\beta$ -sheet type (Fig. 2(b)), although an upward shift of the 1616 cm<sup>-1</sup> band to 1625 cm<sup>-1</sup> has occurred. This shift is also seen in the deconvoluted spectrum, where a strong peak at 1627 cm<sup>-1</sup> is characteristic of intramolecular H-bonding within an anti-parallel  $\beta$ -sheet structure [17]. The result of the GCF in Table 1



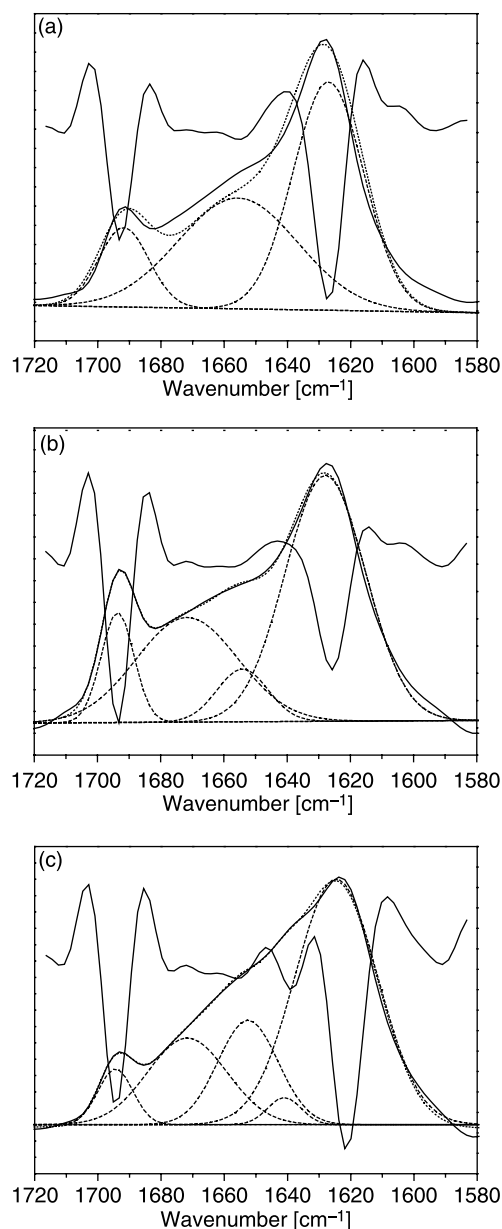


Fig. 2. Amide I spectra of spray-dried PLS powders obtained from different liquid feeds. In each figure the curves are as described in the Fig. 1. (a) Solid obtained from  $\alpha$ -helix liquid feed; (b) solid obtained from  $\beta$ -sheet liquid feed; (c) solid obtained from random coil liquid feed. Fig. 3 Amide I spectra of re-dissolved PLS spray-dried powders. In each figure the curves are as described in the Fig. 1. (a) Re-dissolved solid from  $\alpha$ -helix liquid feed; (b) re-dissolved solid from  $\beta$ -sheet liquid feed; (c) re-dissolved solid from random coil liquid feed.

shows 53% intensity for the  $1627\text{ cm}^{-1}$  band, greatly increased over the 30% intensity for the intermolecular  $1617\text{ cm}^{-1}$  band in the liquid feed. The coupled high-frequency band at  $1691/1693\text{ cm}^{-1}$  stays unchanged at 9% relative intensity. The strong  $1642\text{ cm}^{-1}$  band in both the deconvoluted and second-derivative spectra of the liquid feed and assigned to residual  $\alpha$ -helix (cf. Fig. 1(b)) has disappeared in both spectra of the spray-dried solid. It has been replaced by increased intensity of the  $1627\text{ cm}^{-1}$   $\beta$ -sheet band and by a small peak at  $1655\text{ cm}^{-1}$  in the deconvoluted spectrum

( $1657\text{ cm}^{-1}$  in the second-derivative spectrum) and resolved by the GCF to give 8% intensity assignable to random coil structure and too far removed from  $1644\text{ cm}^{-1}$  to be  $\alpha$ -helix. This is the same behavior observed with the  $\alpha$ -helix liquid feed, where spray-drying caused complete loss of the  $\alpha$ -helix band at  $1644\text{ cm}^{-1}$  and formation of anti-parallel  $\beta$ -sheet at  $1627\text{ cm}^{-1}$  and random coil at  $1655\text{ cm}^{-1}$  (cf. Fig. 2(a)). The presence of unwanted  $\alpha$ -helix fraction in the  $\beta$ -sheet liquid feed is therefore fortuitous, since it demonstrates the same band perturbations in this mixture as in the pure  $\alpha$ -helix liquid feed. The GCF also resolves a further band at  $1673\text{ cm}^{-1}$  that is unchanged in relative intensity over that seen in the liquid feed (cf. Fig. 2(a)) and attributed to non-H-bonded amide groups within turn structures [16]. The  $\beta$ -sheet character of the liquid feed is therefore retained in the spray-dried solid, yet at a higher intensity of approximately 62% compared with 38% in the liquid feed (Table 1). This reason for this increased intensity is, however, simply the loss of the  $1642\text{ cm}^{-1}$   $\alpha$ -helix band seen in the heterogeneous liquid feed that is mostly converted to  $1627\text{ cm}^{-1}$   $\beta$ -sheet band. Of interest is the upward shift in wavenumber of the low-frequency  $\beta$ -sheet band that is clearly seen in both the deconvoluted and second-derivative spectra. This indicates that a heated, aqueous pH 11.5 solution of PLS contains intermolecularly H-bonded, extended, denatured PLS chains that are converted to intramolecularly H-bonded anti-parallel  $\beta$ -sheets on spray drying.

The second-derivative spectrum of the spray dried solid obtained from the random coil liquid feed shows characteristic anti-parallel  $\beta$ -sheet coupled bands at  $1621$  and  $1694\text{ cm}^{-1}$  (Fig. 2(c)). A small band at  $1640\text{ cm}^{-1}$  is close to  $\alpha$ -helix (expected at  $1644\text{ cm}^{-1}$ ), and that at  $1656\text{ cm}^{-1}$  is close to random coil (expected at  $1650\text{ cm}^{-1}$ ). The deconvoluted spectrum clearly shows the two  $\beta$ -sheet peaks at  $1625$  and  $1694\text{ cm}^{-1}$ , as well as indications of peaks at approximately  $1640$  and  $1650\text{ cm}^{-1}$ . The GCF resolves band intensities of 56 and 5.4% at  $1625$  and  $1694\text{ cm}^{-1}$ , respectively (Table 1). As already seen with the spray-dried solids obtained from the  $\alpha$ -helix and  $\beta$ -sheet liquid feeds, the strong  $1625$ – $1627\text{ cm}^{-1}$  band corresponds to intermolecular H-bonding in an anti-parallel  $\beta$ -sheet structure in the solid state [17]. The resolved band at  $1653\text{ cm}^{-1}$  of 17.3% relative intensity is assigned to residual random coil, and the small, negligible band at  $1641\text{ cm}^{-1}$  to  $\alpha$ -helix. The result of the GCF in Table 1 yields therefore a spray-drying-induced change from 100% random coil to 61%  $\beta$ -sheet and 17% residual random coil in the spray-dried solid. Spray-drying induces therefore a strong partial loss in random coil structure which is transformed to  $\beta$ -sheet.

Both the initial  $\alpha$ -helix and random coil bands in the deconvoluted and second-derivative spectra of the liquid feeds convert therefore to predominantly intermolecular  $\beta$ -sheet bands in the solid after spray-drying. This means that the intramolecular H-bonds of these two starting structures undergo major reorientation to form intramolecular H-bonds within an anti-parallel  $\beta$ -sheet structure. The causes of this reorientation are the removal of water molecules from the vicinity of the globular PLS-molecule's surface and the spatial

approach of the PLS-molecules to one another in the solid state being formed. The former effect must be associated with the loss of intermolecular H-bonds between the PLS's peptide chain (amide groups) or side chains (carboxyl groups) and the water dipole. This idea is corroborated by band shift in the  $\beta$ -sheet liquid feed from intermolecular H-bonded extended chains to intramolecular H-bonded anti-parallel  $\beta$ -sheet on spray-drying. This general shift to anti-parallel  $\beta$ -sheet in the dried state occurs because of its stronger H-bonds, that reduce the degree of solvation of the polypeptide chains compared with  $\alpha$ -helix or random coil [6]. Although the H-bonds of the denatured, extended chain structure are stronger than those of the  $\beta$ -sheet structure [16], this does not prevent transition of the former to the latter on spray-drying the  $\beta$ -sheet liquid feed. These results—although more detailed—agree with changes observed in the second-derivative spectra of freeze-dried PLS by Prestrelski et al. [4]. These authors concluded that the preferred conformation of PLS in the freeze-dried state is  $\beta$ -sheet, regardless of its initial conformation in aqueous solution. Spray-drying gives the same result, although our analysis of both FSD and second-derivative spectra combined with GCF gives a more differentiated picture for the three liquid feeds. There is therefore no sign that a very rapid drying-rate reduces or inhibits the conformational change of PLS, as had been proposed by Volkers et al. [7].

The spray-drying-induced changes are to a large extent reversible on re-dissolution of the powders. Fig. 3(a) shows the second derivative spectrum of the re-dissolved powder obtained from the  $\alpha$ -helix liquid feed. A predominant band at  $1646\text{ cm}^{-1}$  is assignable to reformed  $\alpha$ -helix conformation. A band at  $1625\text{ cm}^{-1}$  could be  $\beta$ -sheet, but there is no coupled, high-frequency band. The deconvoluted spectrum is visually very similar in shape to that of the liquid feed (cf. Fig. 1(a)) and shows a broad band at  $1645\text{ cm}^{-1}$  assignable to reformed  $\alpha$ -helix conformation [4]. The GCF resolves three bands at  $1645\text{ cm}^{-1}$  ( $\alpha$ -helix),  $1620\text{ cm}^{-1}$  ( $\beta$ -sheet), and  $1676\text{ cm}^{-1}$  (assignable to non-H-bonded amide groups within turn structures [16]) which agree with those seen in the second derivative spectrum. We treat, however, both the  $1620$  and  $1676\text{ cm}^{-1}$  bands with circumspection, as they are not obvious in the deconvoluted spectrum, despite the slightly broader band shape in Fig. 3(c) compared with Fig. 3(a). To be certain of its existence a band should be distinguishable in both the deconvoluted and second-derivative spectra [16,17]. In this case, Table 1 yields complete reformation of the initial  $\alpha$ -helix structure on re-dissolution of the solid that contained 0%  $\alpha$ -helix after spray drying. Should the  $1620\text{ cm}^{-1}$  really exist, then some  $\beta$ -sheet structure present in the spray-dried solid remains so after re-dissolution. Whatever the case, the spray-drying induced alteration in the amide I band from  $\alpha$ -helix to intramolecular  $\beta$ -sheet plus random coil is therefore largely reversed on re-dissolution.

The spectra of the re-dissolved powder obtained from the  $\beta$ -sheet liquid feed are shown in Fig. 3(b). The major band in the second-derivative spectrum lies at  $1616\text{ cm}^{-1}$  with the coupled high-frequency band at  $1691\text{ cm}^{-1}$ . This indicates reformation of extended, denatured polypeptide chains with strong intermolecular H-bonding. There is no reappearance of

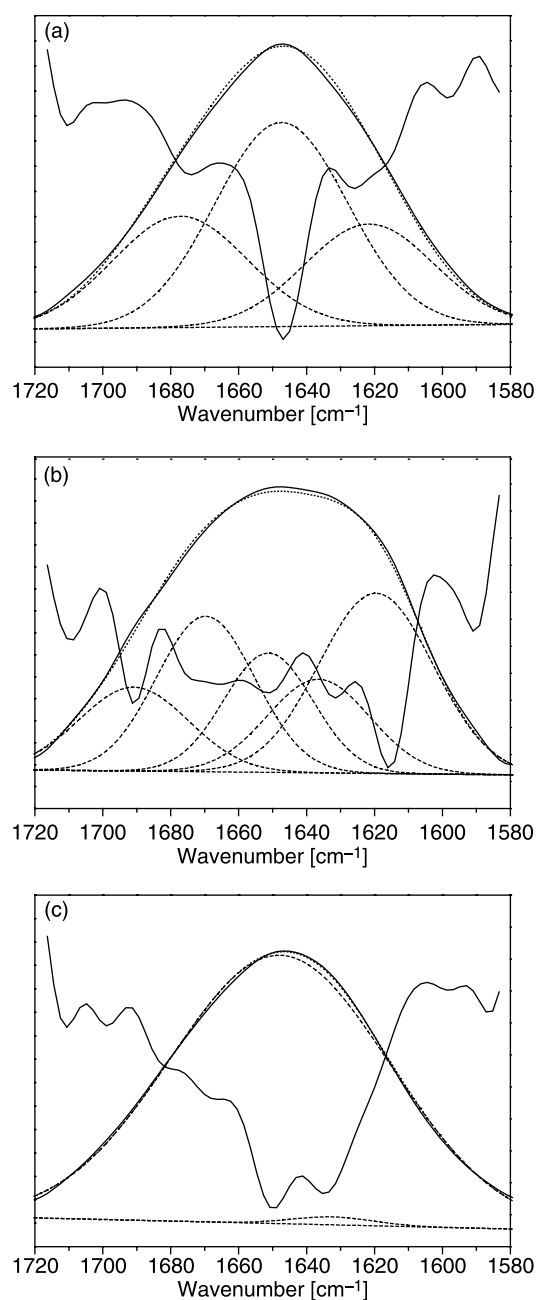


Fig. 3. Amide I spectra of spray-dried PLS/treh powders. (a) Second derivative spectra of spray-dried PLS/treh with  $w_{\text{PLS/treh}} = (2:8)-(9:1)$  prepared from  $\alpha$ -helix liquid feed; (b) second derivative spectra of spray-dried PLS/treh with  $w_{\text{PLS/treh}} = (2:8)-(9:1)$  prepared from random coil liquid feed; (c) second derivative spectra of spray-dried PLS/treh with  $w_{\text{PLS/treh}} = (2:8)-(8:2)$  prepared from  $\beta$ -sheet liquid feed; (d) curve-fitted, deconvoluted original spectrum of PLS/treh  $w_{\text{PLS/treh}} = (8:2)$  prepared from  $\alpha$ -helix liquid feed; (e) curve-fitted, deconvoluted original spectrum of PLS/treh  $w_{\text{PLS/treh}} = (2:8)$  prepared from  $\alpha$ -helix liquid feed; (f) curve-fitted, deconvoluted original spectrum of PLS/treh  $w_{\text{PLS/treh}} = (6:4)$  prepared from random coil liquid feed.

the  $\alpha$ -helix band seen at  $1642\text{ cm}^{-1}$  in the liquid feed, but absent in the spray dried solid. Other bands are evident at  $1636$ ,  $1650$ , and  $1670\text{ cm}^{-1}$ . An assignment of these bands is, however, equivocal, since the deconvoluted spectrum in Fig. 3(b) shows only a single, very broad band with no clearly distinguishable peaks. The same problem occurs

with the five bands resolved by the GCF at  $1616\text{ cm}^{-1}$  (intermolecular H-bonding in extended polypeptide chains),  $1631\text{ cm}^{-1}$  (anti-parallel  $\beta$ -sheet [17]),  $1651\text{ cm}^{-1}$  (random coil),  $1670\text{ cm}^{-1}$  (non-H-bonded amide groups within turn structures [16]), and  $1691\text{ cm}^{-1}$  (coupled, high-frequency inter- or intramolecular H-bonding). The assignment is not justifiable because of the lack of correlation between FSD and second-derivative spectra. From the evidence of the second-derivative spectrum, however, re-dissolution of the solid causes its anti-parallel  $\beta$ -sheet structure to revert to extended chain in solution. Additionally, the solid's fraction of anti-parallel  $\beta$ -sheet formed from the  $\alpha$ -helix structure initially present in the liquid feed, remains as anti-parallel  $\beta$ -sheet after re-dissolution. There is therefore no reformation of this  $\alpha$ -helix band on re-dissolution according to both the second derivative spectrum and the GCF result. Spray-drying causes therefore a reversible change of the intermolecular H-bonding band at  $1617\text{ cm}^{-1}$  of the extended, denatured chains of PLS in this liquid feed.

For the initial random coil liquid feed, re-dissolution of the spray-dried powder reforms a random coil band at  $1649\text{ cm}^{-1}$  in the second-derivative spectrum (Fig. 3(c)) accompanied by a second band at  $1633\text{ cm}^{-1}$ . The deconvoluted spectrum shows, however, almost complete restoration of the strong random coil band at  $1648\text{ cm}^{-1}$ . The GCF resolves this band (Table 1) as 98% random coil, and also the very weak second band at  $1633\text{ cm}^{-1}$  (anti-parallel  $\beta$ -sheet) with 2% intensity.

Both the initial  $\alpha$ -helix and random coil liquid feeds show therefore on re-dissolution almost completely reversibility of the spray-drying-induced changes in their amide I spectra. Similarly, the spray-drying-induced alterations of the extended, denatured polypeptide chains of the  $\beta$ -sheet liquid feed are also reversible. The non-reversible changes observed on spray drying and re-dissolution of this liquid feed come from the contaminating  $\alpha$ -helix fraction present. A visual comparison of the spectra of the liquid feeds (Fig. 1(a)–(c)) with those of the re-dissolved powders (Fig. 3(a)–(c)) reveals an alteration on spray-drying plus re-dissolution to less clearly-defined bands, especially in the second-derivative spectra. This indicates greater heterogeneity of H-bonding in the re-dissolved powders, which means that spray-drying must cause some permanent perturbations in interactions within and between the polypeptide chains of the PLS.

### 3.2. Poly-L-lysine plus Trehalose

Prestrelski et al. [4] reported that sucrose inhibited the transition of the second-derivative spectrum of PLS from random coil to  $\beta$ -sheet during freeze-drying, although no details of sucrose concentration or band shifts were given. Fig. 4(a) shows the effects of increasing weight ratio of trehalose (treh) on the second derivative spectra of spray-dried PLS/treh mixtures prepared from the  $\alpha$ -helix liquid feed. Recall from Fig. 2(a) that the second-derivative spectrum of the spray-dried, pure PLS showed anti-parallel  $\beta$ -sheet bands at  $1627$  and  $1693\text{ cm}^{-1}$ , plus a weak random coil band at  $1655\text{ cm}^{-1}$  and no residual  $\alpha$ -helix band at  $1644\text{ cm}^{-1}$ .

Increasing the PLS/treh weight ratio,  $w_{\text{PLS/treh}}$ , from (1:0) to (4:6) does not produce any substantial change in the second-derivative spectrum of the solids (Fig. 4(a)). At  $w_{\text{PLS/treh}} \geq (3:7)$ , however, a prominent band at  $1650\text{ cm}^{-1}$  appears. We assign this band to random coil structure, since the wavenumber agrees with that found in the random coil liquid feed and is far enough removed from the  $1644\text{ cm}^{-1}$  expected for  $\alpha$ -helix. The deconvoluted spectra of the spray-dried solids containing up to  $w_{\text{PLS/treh}} = (4:6)$  differ little from that for the pure PLS shown in Fig. 2(a). Fig. 4(d) shows, by way of example, the deconvoluted spectrum obtained from the  $w_{\text{PLS/treh}} = (8:2)$  solid, in which peaks are evident at  $1623\text{ cm}^{-1}$  (anti-parallel  $\beta$ -sheet),  $1652\text{ cm}^{-1}$  (random coil) and  $1693\text{ cm}^{-1}$  ( $\beta$ -sheet transition dipole coupling). The GCF resolves the same three bands, plus an additional, small band at  $1675\text{ cm}^{-1}$  that can be assigned to non-H-bonded amide groups within turn structures [16] but is not evident in the second-derivative spectrum of this composition. The quantitative result of the GCF is given in Table 2 and yields 63%  $\beta$ -sheet ( $1625$  and  $1693\text{ cm}^{-1}$  bands) and 32% random coil ( $1652\text{ cm}^{-1}$  band), quite similar to the 59%  $\beta$ -sheet and 41% random coil in the spray-dried, pure PLS (cf. Table 1). The addition of up to 6 weight-parts trehalose to 4 weight-parts PLS (i.e.  $w_{\text{PLS/treh}} = (4:6)$ ) has therefore only a marginal influence on the deconvoluted and second-derivative spectra of the spray-dried solid and does not prevent the spray-drying-induced total loss of the initial  $\alpha$ -helix band at  $1644\text{ cm}^{-1}$ . The dramatic increase in intensity at  $w_{\text{PLS/treh}} \geq (3:7)$  of the  $1650\text{ cm}^{-1}$  band in the second derivative spectrum (Fig. 4(a)) is mirrored in the deconvoluted spectrum shown in Fig. 4(e)) for the example of  $w_{\text{PLS/treh}} = (2:8)$ . The  $1651\text{ cm}^{-1}$  peak is now clearly much more intense than either of the  $\beta$ -sheet peaks at  $1624$  and  $1692\text{ cm}^{-1}$ . The GCF resolves the large band at  $1648\text{ cm}^{-1}$ , the much smaller anti-parallel  $\beta$ -sheet band at  $1624\text{ cm}^{-1}$  with transition dipole coupling at  $1692\text{ cm}^{-1}$ , and also a  $1677\text{ cm}^{-1}$  band assignable to non-H-bonded amide groups within turn structures [17] that is also evident in both the deconvoluted and second-derivative spectra of this composition. The quantitative result for secondary structure in Table 2 gives 18%  $\beta$ -sheet and 59% random coil, which is less  $\beta$ -sheet and more random coil than the 59%  $\beta$ -sheet and 41% random coil for the spray-dried, pure PLS (cf. Table 1). Up to eight weight-parts trehalose to two weight-parts PLS (i.e.  $w_{\text{PLS/treh}} = (2:8)$ ) also does not prevent the total loss of the initial  $\alpha$ -helix band in both the deconvoluted and second-derivative spectra at  $1644\text{ cm}^{-1}$ . No stabilizing effect of the trehalose on the initial  $\alpha$ -helix band of the PLS during spray-drying is seen. The trehalose does, however, give improved recovery of the  $\alpha$ -helix band on re-dissolution of the spray dried powders. At all values of  $w_{\text{PLS/treh}}$  between (1:0) and (2:8) the deconvoluted and second-derivative spectra (not shown) show a reformed, strong band at  $1644$ – $1646\text{ cm}^{-1}$ . Recall from Table 1 that the re-dissolved pure PLS powder from the  $\alpha$ -helix liquid feed showed equivocal spectra, indicating 49% reformed  $\alpha$ -helix. With all of the PLS/treh mixtures the spectra are in agreement with each other, and the GCF yields reformation of  $\geq 80\%$  of the  $\alpha$ -helix band at  $1646/1644\text{ cm}^{-1}$  (Table 2) accompanied by small bands at

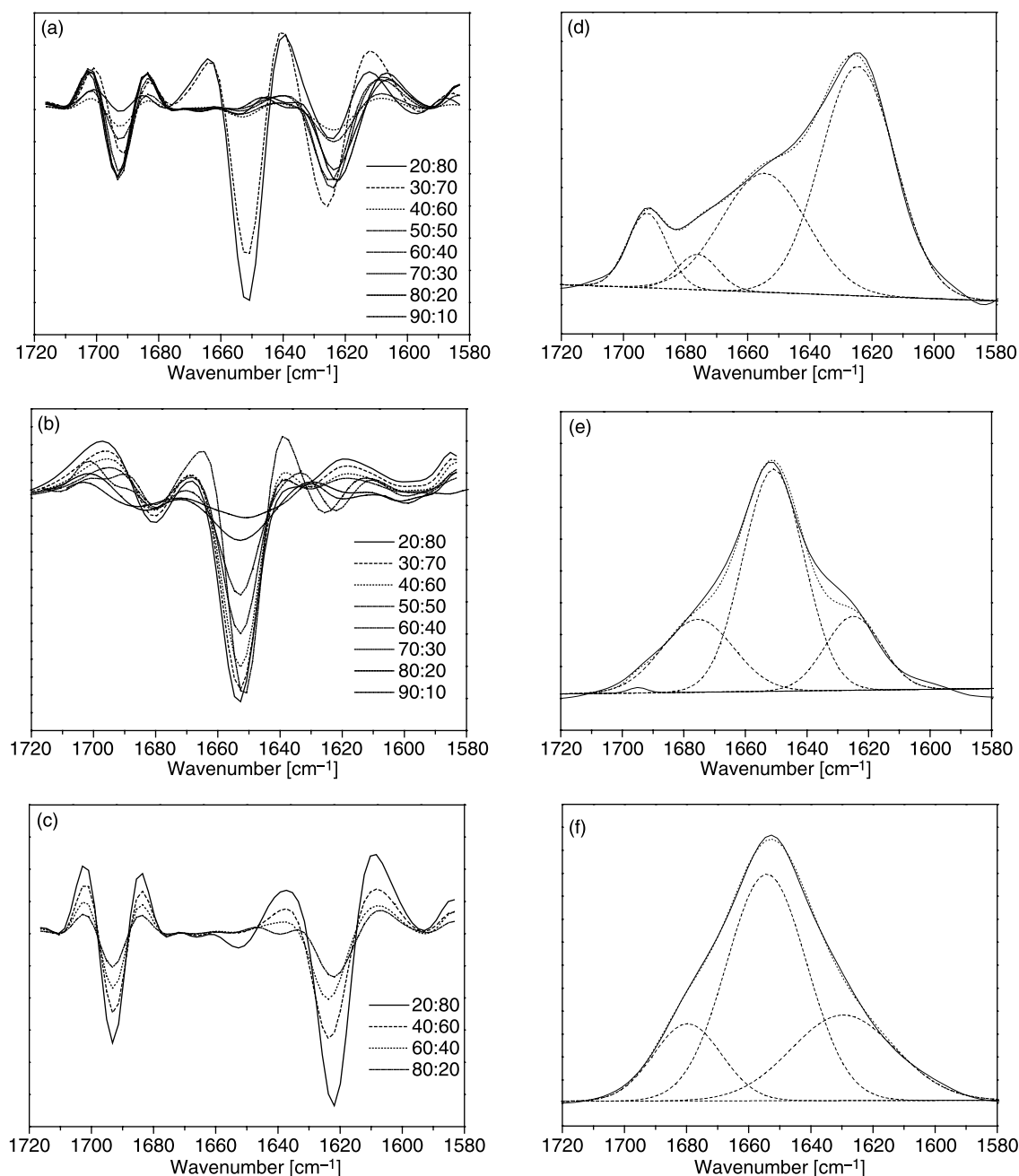


Fig. 4. Amide I spectra of spray-dried PLS/treh powders. (a) Second derivative spectra of spray-dried PLS/treh with  $w^{\text{PLS/treh}} = (2:8) - (9:1)$  prepared from  $\alpha$ -helix liquid feed. (b) Second derivative spectra of spray-dried PLS/treh with  $w^{\text{PLS/treh}} = (2:8) - (9:1)$  prepared from random coil liquid feed. (c) Second derivative spectra of spray-dried PLS/treh with  $w^{\text{PLS/treh}} = (2:8) - (8:2)$  prepared from  $\beta$ -sheet liquid feed. (d) Curve-fitted, deconvoluted original spectrum of PLS/treh  $w^{\text{PLS/treh}} = (8:2)$  prepared from  $\alpha$ -helix liquid feed. (e) Curve-fitted, deconvoluted original spectrum of PLS/treh  $w^{\text{PLS/treh}} = (2:8)$  prepared from  $\alpha$ -helix liquid feed. (f) Curve-fitted, deconvoluted original spectrum of PLS/treh  $w^{\text{PLS/treh}} = (6:4)$  prepared from random coil liquid feed

1615/1616  $\text{cm}^{-1}$  (extended, denatured polypeptide chains [16]) and 1690/1691  $\text{cm}^{-1}$  ( $\beta$ -sheet transition dipole coupling).

In contrast to the result with the  $\alpha$ -helix liquid feed, a moderate stabilizing effect of trehalose is seen with spray-dried PLS/treh prepared from the random coil liquid feed. Recall that the second-derivative spectrum of the pure, spray-dried PLS (cf. Fig. 2(c)) shows  $\beta$ -sheet bands at 1625 and 1694  $\text{cm}^{-1}$  and a smaller residual random coil band at 1656  $\text{cm}^{-1}$ . Twenty parts by weight of added trehalose ( $w_{\text{PLS/treh}} = 8:2$ ) have

already reduced the  $\beta$ -sheet bands in the second derivative spectrum (Fig. 4(b)). With  $w_{\text{PLS/treh}} (3:7)$  the random coil band at 1650–1652  $\text{cm}^{-1}$  progressively dominates the spectrum, although the  $\beta$ -sheet bands lying between 1617 and 1625  $\text{cm}^{-1}$  and at 1680  $\text{cm}^{-1}$  remain present. The deconvoluted spectrum of the system  $w_{\text{PLS/treh}} = (6:4)$  shown in Fig. 4(f) is representative of these changes and is substantially different from that of the pure PLS in Fig. 2(c). It is evidently comprised of a strong peak at 1653  $\text{cm}^{-1}$  that we assign to random coil, and much weaker  $\beta$ -sheet peaks recognizable as shoulders at



Table 2  
Gaussian curve fitting (GCF) of amid I spectra of PLS/treh spray-dried solids and re-dissolved powders

System	Liquid feed	Peak Nr.	Wavenumber GCF (cm <sup>-1</sup> )	Wavenumber 2nd derivative (cm <sup>-1</sup> )	$\alpha$ -helix (%)	$\beta$ -sheet (%)	Random coil (%)	other (%)
(80:20) SD	Random coil	1	1681	1683		23		
		2	1653	1652			55	
		3	1618	1617		21		
		Total				44	55	
(80:20) Re-dissolved	Random coil	1	1646	1648			100	
		Total					100	
(40:60) SD	Random coil	1	1680	1680		18		
		2	1654	1652			54	
		3	1630	1629		28		
						46	54	
(40: 60) Re-dissolved	Random coil	1	1649	1649			94	
		2	1632	1631		5.8		
						5.8	94	
(20:80) SD	Random coil	1	1680	1679		21		
		2	1655	1652			49	
			1633	1633		30		
(20:80) Re-dissolved	Random coil	1	1647	1649			98	
		2	1637	1635		1.7		
						1.7	98	
(80:20) SD	$\alpha$ -helix	1	1692	1693		9		
		2	1676	1675				5
		3	1655	1652			32	
		4	1625	1623		54		
						63	32	5
(80: 20) Re-dissolved	$\alpha$ -helix	1	1690	1691		3.0		
		2	1642	1644	90			
		3	1616	1615		7		
					90	10		
(40:60) SD	$\alpha$ -helix	1	1693	1693		3		
		2	1673	1675				28
		3	1652	1650			18	
		4	1627	1624		51		
						54	18	28
(40.60) Re-dissolved	$\alpha$ -helix	1	1691	1691		5		
		2	1645	1646	94			
		3	1618	1619		1		
					94	6		
(20:80) SD	$\alpha$ -helix	1	1695	1692		0.4		
		2	1676	1677				23
		3	1651	1648			59	
		4	1625	1624		18		
(20: 80) Re-dissolved	$\alpha$ -helix	1	1687	1690		18.4	59	23
		2	1646	1646	80	10		
		3	1616	1616		10		
					80	20		
(80: 20) SD	$\beta$ -sheet	1	1693	1693		7		
		2	1671	1675				16
		3	1651	1654			17	
		4	1640	1639		4		
		5	1624	1621		56		
(80. 20) Re-dissolved	$\beta$ -sheet					67	17	16
		1	1691	1691		10		
		2	1662	1659				39
		3	1632	1631		36		
		4	1616	1616		15		
(40: 60) SD	$\beta$ -sheet	1	1692	1693		9		
		2	1676	1675				6
		3	1655	1654			30	
		4	1625	1623		56		
						65	30	6

(continued on next page)

Table 2 (continued)

System	Liquid feed	Peak Nr.	Wavenumber GCF (cm <sup>-1</sup> )	Wavenumber 2nd derivative (cm <sup>-1</sup> )	$\alpha$ -helix (%)	$\beta$ -sheet (%)	Random coil (%)	other (%)
(40: 60) Re-dissolved	Sheet	1	1688	1690		12		
		2	1670	1671				19
		3	1657	1651			19	
		4	1644	1633				
		5	1624	1618		46		
(20: 80) SD	$\beta$ -sheet					58	19	25
		1	1693	1693		9		
		2	1674	1675				11
		3	1652	1652			32	
		4	1623	1622		48		
(20: 80) Re-dissolved	$\beta$ -sheet					57	32	11
		1	1691	1691		1		
		2	1662	1662				46
		3	1631	1636		46		
		4	1617	1616		7		
						54		46

approximately 1625 and 1680 cm<sup>-1</sup>. The GCF resolves these three bands with intensities of 46% spray-drying-induced  $\beta$ -sheet and 54% retained random coil, compared with 61% induced  $\beta$ -sheet and 17% retained random coil in the pure spray-dried PLS (cf. Table 1). With increasing weight-proportion of trehalose up to  $w_{\text{PLS/treh}} = (2:8)$  no further change in the deconvoluted spectra or the GCF intensities of the bands occurs. This is seen despite the evident increasing relative intensity of the 1653 cm<sup>-1</sup> band in the second-derivative spectra of Fig. 4(b). Band intensity in a second-derivative plot is, however, determined by the rate of change of the dependent variable (i.e. absorbance) in the original plot and not its absolute intensity. Differing band intensities in a second derivative amide I spectrum are therefore not an accurate measure of the intensities of the bands in the original deconvoluted spectrum [16,17]. The addition of up to two weight-parts trehalose to eight parts PLS causes therefore a substantial increase in the amount of retained initial random coil conformation on spray drying from 17 to 54%, although only a modest reduction in the amount of  $\beta$ -sheet formed is seen. On re-dissolution of these spray-dried solids a complete reformation of the random coil band is obtained with all PLS/treh mixtures (Table 2), as had been seen before with the pure PLS (cf. Table 1).

Recall that the PLS from the  $\beta$ -sheet liquid feed showed retention of  $\beta$ -sheet-type second derivative and deconvoluted spectra after spray-drying. An upward shift in wavenumber indicated, however, that an initial extended chain structure in the liquid feed is transformed to anti-parallel  $\beta$ -sheet in the dried solid. The same behavior is found with all of the PLS/treh mixtures. The second derivative spectra in Fig. 4(c) illustrate how with increasing weight proportion of trehalose the bands at approximately 1623 cm<sup>-1</sup> (anti-parallel  $\beta$ -sheet) and 1693 cm<sup>-1</sup> ( $\beta$ -sheet transition dipole coupling) remain the dominant features of the spectrum of each spray-dried solid. The trehalose does not therefore prevent the transformation of extended chain to anti-parallel  $\beta$ -sheet structure in the solid state. The deconvoluted spectra (not shown, for brevity) also

show minimal alteration with change in  $w_{\text{PLS/treh}}$ . The GCF results in Table 2 show for the example of the  $w_{\text{PLS/treh}} = (8:2)$  system a secondary structural composition of 66% anti-parallel  $\beta$ -sheet and 17% random coil in the spray-dried powder, essentially the same as the 62% anti-parallel  $\beta$ -sheet and 8% random coil of the spray-dried pure PLS (Table 1). This also means that the trehalose does not prevent conversion of the  $\alpha$ -helix fraction present in the  $\beta$ -sheet liquid feed (approximately 30%, Fig. 1(a) and Table 1) to anti-parallel  $\beta$ -sheet on spray-drying. This is, however, the same behavior seen with the  $\alpha$ -helix liquid feed, which is completely transformed to  $\beta$ -sheet and random coil on spray-drying and not stabilized by the addition of trehalose. Further increase in  $w_{\text{PLS/treh}}$  to (2:8) produces minimal change in the quantitative analysis of the GCF (Table 2). The addition of up to 80 weight-parts trehalose to 20 weight-parts PLS does not therefore prevent the spray-drying-induced shift of the initial 1616 cm<sup>-1</sup> band to 1623 cm<sup>-1</sup>, indicative of the conversion of denatured, extended chains to anti-parallel  $\beta$ -sheet. Such a transition involves, however, a change from strong intermolecular H-bonds in the extended, solvated chains [16] to weaker, intramolecular H-bonds in the anti-parallel  $\beta$ -sheet of the solid.

The ‘stabilizing’ action of trehalose on the amide I bands is thus different for the three initial conformations. It reduces the extent of loss of a random coil conformation, but cannot prevent complete loss of an  $\alpha$ -helix conformation nor transformation of intermolecular to intramolecular H-bonding in  $\beta$ -sheet structures on spray drying. Assuming that trehalose interacts with PLS during spray-drying via ‘water replacement’, then the difference in behavior may be explained by differing H-bonding patterns and strengths of the conformations. The random coil conformation of PLS in aqueous solution has weak intermolecular H-bonds between the polypeptide amide or side chain carboxyl groups and surrounding water molecules [15] resulting in a high wavenumber of amide I absorption at 1650 cm<sup>-1</sup> (non-H-bonded amide groups absorb at approximately 1666 cm<sup>-1</sup> [21]). If drying proceeds sufficiently to cause removal of these

water molecules from the ‘surface’ of the PLS molecule, then some of these amide/carboxyl groups become available to form new intermolecular H-bonds with the -OH groups of the trehalose molecules that are approaching the PLS molecule’s surface. These new H-bonds are sufficiently strong to maintain partially a random coil structure of the PLS in the dried state, and reduce therefore the likelihood that the random coil transforms to  $\beta$ -sheet on water loss. No specific intramolecular H-bonds need to be stabilized to maintain the random coil structure. In contrast, the  $\alpha$ -helix conformation of PLS is structurally maintained by well-defined, strong intramolecular H-bonds of the polypeptide chain’s amide groups [22] and, additionally, has strong intermolecular H-bonds with water at the PLS molecule’s surface [23]. The wavenumber of amide I absorption is therefore lower— $1646\text{ cm}^{-1}$ —than that of the random coil structure [16]. The removal of these water molecules from the PLS molecule’s ‘surface’ during drying results in loss of the  $\alpha$ -helix structure for one, or both, of two possible reasons. First, the approaching trehalose molecules cannot H-bond to the side-chain carboxyl groups presented at the PLS molecule’s surface. Although the outside helix surface is hydrophobic [22], H-bonding to  $\alpha$ -helix side chains is strong [6], making this mechanism unlikely. Secondly, the H-bonding of the trehalose molecules to the side-chain carboxyl groups is insufficient to maintain the specific, well-defined intramolecular H-bonds that hold together the  $\alpha$ -helix structure. The specific, well-defined intramolecular H-bonds in the  $\alpha$ -helix structure are more sensitive to the destruction of the intermolecular H-bonds on the PLS molecule’s surface during drying than are the unspecific intramolecular H-bonds in the random coil state. Indeed, at high trehalose weight-fractions ( $w_{\text{PLS/treh}} \geq 7:3$ ) the  $\alpha$ -helix is transformed partly to random coil on spray drying (Fig. 4(a)) which can be more readily stabilized by intermolecular H-bonds with the trehalose than can the  $\alpha$ -helix. ‘water replacement’ with trehalose is therefore incapable of preventing the spray-drying-induced shift to  $\beta$ -sheet. The  $\alpha$ -helix configuration cannot be stabilized at any of the weight fractions of added trehalose examined here. Similar behavior is shown by the  $\beta$ -sheet conformation. The extended chain structure is characterized by strong, intermolecular H-bonds between the amide groups of adjacent chains [16] resulting in the low wavenumber of absorption— $1616\text{ cm}^{-1}$ —measured in the  $\beta$ -sheet liquid feed (cf. Fig. 1(b)). Water molecules are less strongly bound to the PLS molecule’s ‘surface’ than in the  $\alpha$ -helix state [6]. The change to anti-parallel  $\beta$ -sheet on spray-drying involves a change from strong intermolecular H-bonds to weaker intramolecular H-bonds. The H-bonding of approaching trehalose molecules to the ‘surface’ of the PLS molecules cannot prevent this change at any of the trehalose weight-fraction examined here. In the dried state, the anti-parallel  $\beta$ -sheet structure is evidently energetically more favorable than either extended chain,  $\alpha$ -helix or random coil. It follows that the factor determining the efficacy of ‘water replacement’ stabilization cannot be H-bond strength alone, otherwise the extended chain would be maintained on a drying. Also, the sensitivity to stabilization by trehalose would be in

the sequence random coil  $< \alpha$ -helix  $< \beta$ -sheet. It is more likely that steric effects, combined with H-bond strength and type, determine the shift to anti-parallel  $\beta$ -sheet on drying. Trehalose can prevent this only when the newly-formed intermolecular H-bonds on the PLS molecule’s surface are sufficient to stabilize the intramolecular H-bonds of the secondary structural element, i.e. with random coil but not  $\alpha$ -helix or extended chain.

#### 4. Conclusions

1. The FT-IR amide I bands of the homopolypeptide PLS when spray-dried at  $T_{\text{in}}/T_{\text{out}} = 130/90\text{ }^{\circ}\text{C}$  and starting from either the  $\alpha$ -helix,  $\beta$ -sheet (extended chain), or random coil configurations shows a shift to anti-parallel  $\beta$ -sheet secondary structure in the resulting solid. This result was obtained by a careful analysis of deconvoluted and second-derivative spectra, combined with Gaussian curve fitting. The anti-parallel  $\beta$ -sheet conformation is energetically the most favorable state in the dried solid. This is not only a result of stronger H-bonds, since the extended chain initial conformation that has the strongest H-bonds, also transforms to anti-parallel  $\beta$ -sheet on spray-drying. Steric effects, e.g. polypeptide chain alignment in the dried state, are suggested as also being a determining factor in the formation of anti-parallel  $\beta$ -sheet on drying. Re-dissolution of the spray-dried powders in water caused reversion to the initial secondary structure before spray-drying.
2. The stabilizing effect of trehalose on the maintenance of the initial secondary structure of the PLS on spray-drying depends on the type of secondary structural element present. The  $\alpha$ -helix and  $\beta$ -sheet, extended chain conformations cannot be stabilized by trehalose at any weight-fraction examined here. Random coil is, however, stabilized to some extent by the addition of up to 20 parts by weight of trehalose to 80 parts peptide. There is therefore no simple relation between H-bond strength and the stabilizing action of trehalose. The ability of trehalose/water intermolecular H-bonds to stabilize the intramolecular H-bonds of the secondary structural element appears to determine the efficacy of the trehalose.
3. The relevance of this work is the finding that spray-drying induced conformational change of poly-L-lysine to  $\beta$ -sheet is not solely a consequence of favored H-bonding. Clearly, any comparison of this behavior of poly-L-lysine with that of proteins must be treated with care. It is evident, however, that drying-induced conformational changes, and their prevention, do depend on the initial structure present. This gives some guidance for work with proteins of complex, mixed secondary structures.

#### Acknowledgements

We are most grateful to the Deutsche Forschungsgemeinschaft in Bonn for their generous financial support (Le 626/7-1) of this project.

## References

- [1] W. Kauzmann, Some factors in the interpretation of protein denaturation, *Adv. Protein Chem.* 14 (1951) 1–63.
- [2] S. Tzannis, S. Prestrelski, Activity–stability considerations of trypsinogen during spray drying: effects of sucrose, *J. Pharm. Sci.* 88 (1999) 349–351.
- [3] Y. Maa, P. Nguyen, C. Hsu, Spray drying of air–liquid interface sensitive recombinant human growth hormone, *J. Pharm. Sci.* 87 (1998) 152–159.
- [4] S. Prestrelski, N. Tedeschi, T. Arakawa, J. Carpenter, Dehydration-induced conformational transitions in proteins and their inhibition by stabilizers, *Biophys. J.* 65 (1993) 661–671.
- [5] M. Jackson, P. Haris, D. Chapman, Conformational transitions in poly (L-lysine): studies using Fourier transformation infrared spectroscopy, *Biochim. Biophys. Acta* 998 (1989) 75–79.
- [6] D. Barlow, P. Poole, The hydration of protein secondary structures, *FEBS Lett.* 213 (1987) 423–427.
- [7] W. Volkers, M. Klisdonk, F. Hoekstra, Dehydration-induced conformational changes of poly-L-lysine as influenced by drying rate and carbohydrates, *Biochim. Biophys. Acta* 1425 (1998) 127–136.
- [8] M. Adler, G. Lee, Stability and surface activity of lactate dehydrogenase in spray-dried trehalose, *J. Pharm. Sci.* 88 (1999) 199–208.
- [9] Y.-H. Liao, M. Brown, T. Nazir, A. Quader, G. Martin, Effects of sucrose and trehalose on the preservation of native structure of spray-dried lysozyme, *Pharm. Res.* 19 (2002) 1847–1853.
- [10] H. Costantino, J. Andya, S. Shire, C. Hsu, Fourier transform infrared spectroscopic analysis of the secondary structure of recombinant humanized immunoglobulin G, *Pharm. Sci.* 3 (1997) 121–128.
- [11] M. Maury, K. Murphy, S. Kumar, A. Mauerer, G. Lee, Spray-drying of proteins: effects of sorbitol and trehalose on aggregation and FT-IR amide I spectrum of an immunoglobulin G, *Eur. J. Pharm. Biopharm.* 59 (2005) 251–261.
- [12] H. Chan, A. Clark, J. Feelay, M. Kuo, S. Lehrman, K. Pikal-Cleland, D. Miller, R. Vehring, D. Lechuga-Ballesteros, Physical stability of salmon Calcitonin spray-dried powders for inhalation, *J. Pharm. Sci.* 83 (2004) 792–804.
- [13] M. Maury, K. Murphy, S. Kumar, L. Shi, G. Lee, Effects of process variables on the powder yield of spray-dried trehalose on a laboratory spray-dryer, *Eur. J. Pharm. Biopharm.* 59 (2005) 566–573.
- [14] C. Wabel, G. Lee, FT-IR, Laser diffractometry and centrifugal studies of lecithin stabilized o/w emulsion. *Proceed. 42nd Int. Conf. Arbeitsgem. Pharm. Verfahrenstechnik*, Mainz, 1996.
- [15] E. Goormaghtigh, V. Cabiaux, Ruysschaert, Secondary structure and dosage of soluble and membrane proteins by attenuated total reflection Fourier transform infrared spectroscopy of hydrated films, *Eur. J. Biochem.* 193 (1990) 490–520.
- [16] M. Jackson, H. Mantsch, The use and misuse of FTIR spectroscopy in the determination of protein structure, *Crit. Rev. Biochem. Mol. Biol.* 30 (2) (1995) 95–120.
- [17] Griebenow K., Santos A., Carrasquillo K., Secondary structure of proteins in the amorphous dehydrated state probed by FTIR spectroscopy, first ed., *Internet J. Vibrational Spec.*, vol. 3.
- [18] T. Miyazawa, The characteristic band of secondary amides at  $3100\text{ cm}^{-1}$ , *J. Mol. Spec.* 4 (1960) 168–172.
- [19] W. Dzwolak, T. Muraki, M. Kato, Y. Taniguchi, Chain-length dependence of  $\alpha$ -helix to  $\beta$ -sheet transition in polylysine: model of protein aggregated studied by temperature-tuned FT-IR spectroscopy, *Biopolymers* 73 (2004) 463–469.
- [20] A. Drake, G. Siligardi, W. Gibbons, Reassessment of the electronic circular dichroism criteria for random coil conformations of poly (L-lysine) and the implications for protein folding and denaturation studies, *Biophys. Chem.* 31 (1988) 143–146.
- [21] M. Jackson, H. Mantsch, Beware of proteins in DMSO, *Biochim. Biophys. Acta* 1079 (1991) 231–235.
- [22] C. Brandon, J. Tooze, *Introduction to Protein structure*, second ed., Garland Publications, NY, 1999. pp. 14–16.
- [23] E. Manas, Z. Getrahn, w. Wright, W. DeGrado, J. Vanderkoss, Infrared spectra of amide groups in helical proteins: evidence for hydrogen bonding between helices and water, *JACS* 122 (2000) 9883–9890.